sustainability

MDPI

Article

Vertical Zonation and Functional Characteristics of Sediments Bacteria in Rural Black-Odorous Waterbodies: A Microbiological Perspective for Sustainable Management

Yanfang Tian [1,2,†], Shuai Lu [1,2,3,†], Hongwei Ren [1,2,4], Jinxia Lu [1,2], Jin Wang [4] and Xiaoling Liu [1,2,*]

[1] State Key Laboratory of Environmental Criteria and Risk Assessment, Chinese Research Academy of Environmental Science, Beijing 100012, China; tian.yanfang@craes.org.cn (Y.T.)
[2] State Environmental Protection Key Laboratory of Estuarine and Coastal Environment, Chinese Research Academy of Environmental Science, Beijing 100012, China
[3] School of Environment and Energy Engineering, Beijing University of Civil Engineering and Architecture, Beijing 100032, China
[4] School of Resources and Environmental Engineering, Hefei University of Technology, Hefei 230009, China
* Correspondence: liuxl@craes.org.cn
† These authors contributed equally to this work.

Abstract

Rural black-odorous waterbodies (RBOWBs) represent a critical environmental challenge in China, yet the vertical stratification of sedimentary bacterial communities and its underlying drivers remain poorly understood. This study combined 16S rRNA gene amplicon sequencing across five sediment depths (0–125 cm) with shotgun metagenomic analysis of surface sediments to investigate bacterial diversity, composition, and functional potential in typical rural black-odorous systems of Dongming County, Shandong Province. Results showed a clear decline in bacterial richness with increasing sediment depth, with the surface layer (0–25 cm) exhibiting 1.2–1.9 times higher diversity than deeper strata. Community composition displayed distinct vertical zonation: Chloroflexi and *Thiobacillus* dominated surface layers and were linked to carbon hydrolysis and desulfurization, whereas *Bacillus* and nitrifying bacteria prevailed in deeper anoxic layers. Metagenomic analysis revealed high genetic potential for carbohydrate metabolism, amino acid biosynthesis, and sulfur-nitrogen cycling, with glycoside hydrolases (GHs) and glycosyl transferases (GTs) being particularly abundant. Statistical correlations identified total phosphorus (TP_1), dissolved oxygen (DO), and pH of the overlying water—rather than sediment intrinsic nutrients—as the primary environmental factors associated with microbial functional stratification. These findings provide a mechanistic understanding of vertical microbial zonation in rural black-odorous sediment and offer a microbiological basis for developing depth-resolved sustainable remediation strategies.

Keywords: rural black-odorous waterbodies; sediment bacteria; vertical zonation; metagenomics; sustainable remediation

Check for updates

Academic Editor: Helvi Heinonen-Tanski

Received: 24 November 2025
Revised: 21 January 2026
Accepted: 29 January 2026
Published: 4 February 2026

Copyright: © 2026 by the authors. Licensee MDPI, Basel, Switzerland. This article is an open access article distributed under the terms and conditions of the Creative Commons Attribution (CC BY) license.

1. Introduction

Black-odorous waterbodies (BOWBs) represent a severe environmental deterioration phenomenon, particularly in rural China where decentralized pollution sources and limited infrastructure complicate management [1]. When pollutants such as domestic sewage and agricultural runoff accumulate, dissolved oxygen is rapidly consumed during microbial degradation of organic matter, accelerating hypoxia or anoxia and facilitating the formation

of blackening substances (e.g., ferrous sulfide) and odorous compounds, such as hydrogen sulfide (H_2S) and volatile organic amines [2,3]. Sediments act as both a long-term sink and a potential source for these pollutants, serving as critical habitats for microbial communities that mediate the exchange of matter and energy between sediments and overlying water, making them essential targets for water quality improvement [4–7].

Sediment microbial communities sensitively reflect subtle changes in aquatic environmental factors. Studies have documented significant shifts in community structure in response to gradients of nutrient loading (N, P) [8,9], organic pollution [10], and heavy metal contamination [11], establishing their role as reliable bioindicators. Their composition and diversity serve as key biological indicators of pollution severity, ecosystem integrity, and stability [8,12]. Studies show that sediment bacterial communities are significantly influenced by overlying water and sediment nutrients, particularly total nitrogen (TN) and TP [12,13]. In severely polluted systems, the resulting persistent hypoxia and accumulation of reduced toxic compounds (e.g., sulfides, ammonia) suppress microbial activity and select for a limited set of survival strategies. This leads to a marked decrease in the abundance and diversity of key functional genes, particularly those involved in aerobic respiration, complete denitrification (*nirK*, *nirS*), dissimilatory sulfate reduction (*dsrB*), and the degradation of complex organic pollutants [10,14]. During black-odorous outbreaks, group such as γ-Proteobacteria and Anaerolineae often dominate, driving pollutant degradation but also contributing to odorous substance production [10]. For example, in urban river sediments, genera like *Dechloromonas* and *Geobacter* are frequently reported for their roles in anaerobic denitrification and metal reduction, directly linking community composition to geochemical cycling [15,16]. Similarly, *Sulfurimonas*, prevalent in hypoxic waters, drives sulfide oxidation, a key process in odor mitigation [17]. Post-remediation, genera like *Pseudomonas* and *Halomonas*—critical for removing nitrogen, organic pollutants, and hydrogen sulfide—often increase in abundance. Studies of urban polluted rivers have revealed significant vertical stratification in sediment bacterial communities, where diversity and functional composition vary markedly along sediment depths (0–35 cm), with species turnover (β~SIM~ = 0.48) dominating vertical beta-diversity patterns [13]. These findings underscore the critical role of vertical microbial zonation in pollutant transformation. Thus, systematically analyzing this stratification and its interactions with environmental drivers is vital for understanding rural black-odor formation mechanisms and informing effective remediation strategies.

However, for RBOWBs—characterized by distinct pollution sources (e.g., agricultural runoff, plant residues) and typically deeper, more stratified sediment profiles—knowledge of microbial vertical zonation and its functional drivers remains scarce. Existing research focuses predominantly on surface sediments or overlying water physicochemical properties, neglecting stratified microbial functional synergy across depths [18,19]. This gap impedes the development of targeted bioremediation strategies for rural ecosystems, where microbial metabolism directly influences blackening and odoring mechanisms [20]. Furthermore, while genera such as *Dechloromonas* and *Geobacter* have been widely reported in urban sediments for their roles in denitrification and metal reduction [15,16], and *Sulfurimonas* is known for sulfur oxidation in hypoxic waters [17], their distribution, abundance, and functional interplay in the distinct context of deep rural sediments are poorly understood.

To address this deficiency, we investigate bacterial communities across depths (0–125 cm) in rural black-odorous sediments of Dongming County, Shandong Province. Using 16S rRNA gene amplicon sequencing for profiling community composition and diversity, coupled with shotgun metagenomic sequencing for deciphering functional potential, along with physicochemical analyses, we (1) quantify vertical variations in community diversity and structure, (2) identify depth-specific pollutant-degrading microbiota, and

(3) elucidate the key environmental drivers of microbial stratification. These insights aim to fill a critical knowledge gap and provide a microbiological foundation for sediment pollution control and ecological restoration in rural ecosystems.

2. Materials and Methods

2.1. Sites Description and Sample Collection

This study was conducted in Dongming County, Shandong Province. Sampling targeted five representative rural black-odorous waterbodies (designated S2, S14, S16, S24, S27), selected based on typical pollution characteristics. To enhance the statistical robustness and representativeness of functional potential analysis, five additional sites (S5, S9, S11, S17, S29) were incorporated, expanding the total number of sampling locations to ten. The five supplementary sites (S5, S9, S11, S17, S29) were selected to balance the representation of the two major pollution sources (domestic sewage vs. agricultural runoff) across the entire sample set. Among these, sites S5, S14, S16, S24, and S29 were primarily influenced by domestic sewage, while S2, S9, S11, S17, and S27 were mainly affected by agricultural nonpoint source pollution. This design aimed to capture a broader range of environmental conditions for a more robust analysis of microbial functional potential, while the original five cored sites provided the necessary depth-resolved samples for analyzing vertical community structure. Site distribution followed waterbody typology: ditch-type RBOWBs were sampled at equidistant points (100 m intervals; one point if length < 100 m), while pond-type RBOWBs used a uniform three-point sampling approach. The geographical distribution of all sampling sites is shown in [21], and their GPS coordinates, sampling date, and sampled depth intervals are listed in Supplementary Table S1.

Fieldwork occurred in August 2021. Overlying water samples were collected in sealed polyethylene bottles. For the five original sites (S2, S14, S16, S24, S27), sediment cores were collected, and the material from each core was divided into five depth intervals: A (0–25 cm), B (25–50 cm), C (50–75 cm), D (75–100 cm), and E (100–125 cm). For these sites, three parallel field cores were collected per point and physically homogenized into a single composite sample per depth interval prior to downstream analysis. In contrast, only surface sediments (0–20 cm) were collected from the five supplementary sites (S5, S9, S11, S17, S29) for metagenomic functional analysis. Approximately 1 kg of sediment from each layer or site was stored in sterile polyethylene bags. All samples were immediately preserved at 4 °C and transported to the laboratory within 24 h.

Overlying water was filtered through 0.45 μm membranes for direct analysis. Sediments were sieved (2 mm nylon mesh) to remove debris (e.g., stones, roots), then split: one subsample stored at −80 °C for microbial analysis, and another air-dried for physicochemical characterization. Notably, sites S2, S24, and S27 yielded sediment from only two layers (A and B) due to depth constraints.

2.2. Physicochemical Analysis

For the overlying water of rural black-odorous waterbodies, key measurement indicators include pH, electrical conductivity (EC), transparency, DO, chemical oxygen demand (COD), ammonia nitrogen (NH_4^+-N), and total phosphorus (TP_1 for overlying water). pH and EC were measured on-site using a portable pH/EC meter (HQ40d, Hach, Loveland, CO, USA). DO was measured on-site with a portable dissolved oxygen meter (Pro20, YSI, Yellow Springs, OH, USA) [22]. Transparency was determined using a standard black-and-white Secchi disk (Ø: 30 cm). COD was analyzed using the dichromate method [23]. Both NH_4^+-N and TP_1 are quantified using ultraviolet-visible spectrophotometry (UV-1800, Shimadzu Corporation, Kyoto, Japan) [24,25].

For sediment samples, key measurement indicators include organic matter (OM), TN, total phosphorus (TP_2 for sediment), and heavy metals such as lead (Pb), cadmium (Cd), copper (Cu), nickel (Ni), zinc (Zn), chromium (Cr), mercury (Hg), and arsenic (As). pH was determined using the electrode potential method. Organic matter was analyzed using the potassium dichromate oxidation method [26]. TN was measured by the Kjeldahl method with acid-base titration. TP_2 was determined using the alkali fusion-molybdenum antimony anti-spectrophotometry method [26,27]. Pb and Cd were analyzed using graphite furnace atomic absorption spectrophotometry (PinAAcle 900T, PerkinElmer, Waltham, MA, USA). Cu, Ni, Zn, and Cr were measured using flame atomic absorption spectrophotometry. Hg was determined using a flow injection mercury analyzer. As was analyzed using inductively coupled plasma mass spectrometry [28,29].

2.3. DNA Extraction, Sequencing, and Bioinformatic Analysis

Total genomic DNA was extracted from all sediment samples using the FastDNA Spin Kit for Soil (MP Biomedicals, Santa Ana, CA, USA). Extraction blank controls (no sediment) were included in each batch to monitor potential contamination.

For bacterial community structure analysis, the hypervariable V3–V4 region of the 16S rRNA gene was amplified with the widely used primer pair 338F (5′-ACTCCTACGGGAGG-CAGCAG-3′) and 806R (5′-GGACTACHVGGGTWTCTAAT-3′) using Taq DNA polymerase (Takara Bio Inc., Shiga, Japan) [30]. PCR amplification was performed in triplicate for each sample, followed by pooling and purification. The resulting amplicons were constructed into libraries using the NEXTFLEX™ Rapid DNA-Seq Kit (Bioo Scientific, Austin, TX, USA). This 16S rRNA gene amplicon sequencing approach was employed to provide high-depth, cost-effective profiling of bacterial community composition and diversity across all sites and depth layers. Library preparation and paired-end sequencing (2 × 300 bp) were performed on an Illumina MiSeq platform by Majorbio Bio-Pharm Technology Co., Ltd. (Shanghai, China).

The 16S rRNA gene sequencing data were processed as follows: raw paired-end reads were first merged, quality-filtered, and demultiplexed. Chimeric sequences were identified and removed. High-quality sequences were then clustered into operational taxonomic units (OTUs) at a 97% similarity threshold using the UPARSE algorithm within USEARCH (v11.0). The taxonomy of each representative OTU sequence was assigned by aligning it against the SILVA 138 SSU rRNA reference database using the RDP classifier (v2.13) with a confidence threshold of 0.7. The resulting OTU table was rarefied to an even sequencing depth per sample for subsequent alpha- and beta-diversity analyses.

To gain deeper insight into the functional potential of the microbiota and metabolic pathways, shotgun metagenomic sequencing was employed on a subset of samples, hereby leveraging the complementary strengths of both approaches. Briefly, qualified genomic DNA was fragmented, and libraries were built using the NEXTFLEX™ Rapid DNA-Seq Kit (Bioo Scientific, Austin, TX, USA). Library quality was assessed using a Qubit fluorometer (Thermo Fisher Scientific, Waltham, MA, USA) for quantification and an Agilent 2100 Bioanalyzer (Agilent Technologies, Santa Clara, CA, USA) for size distribution analysis. Qualified libraries were subjected to paired-end sequencing (2 × 150 bp) on an Illumina NovaSeq 6000 platform using an S4 flow cell by Majorbio Bio-Pharm Technology Co., Ltd. (Shanghai, China), with a target output of approximately 15 Gb of raw data per sample.

Bioinformatic processing of the metagenomic data entailed a series of rigorous steps. Raw sequencing reads were first subjected to quality control and adapter trimming using Fastp (version 0.20.0) to obtain clean data [31]. These high-quality reads from each sample were then assembled de novo into contigs using MEGAHIT (version 1.1.2) [32]. Open Reading Frames (ORFs) were predicted from the assembled contigs using Prodigal (v2.6.3), and

the resulting protein sequences were clustered with CD-HIT to construct a non-redundant gene catalog [33]. Gene abundance for each sample was accurately quantified by mapping the clean reads back to this non-redundant catalog using SOAPaligner (version 2.21; SOAP Co., Ltd., BGI, Shenzhen, China). Abundances were normalized and expressed using the RPKM (Reads Per Kilobase per Million mapped reads) method.

Functional annotation of the predicted genes was performed to decipher their metabolic roles. Non-redundant protein sequences were aligned against the Kyoto Encyclopedia of Genes and Genomes (KEGG) database using Diamond (v2.0.13) with a blastp search strategy (E-value $\leq 1 \times 10^{-5}$) to map genes to biological pathways [34]. Concurrently, carbohydrate-active enzymes were identified by comparing sequences to the CAZy database using HMMER (v3.1b2), providing specific insights into the community's carbohydrate metabolism capabilities [35].

2.4. Statistical Analysis

Bioinformatic processing was conducted on the Majorbio Cloud Platform (Majorbio Bio-pharm Technology Co., Ltd., Shanghai, China). For the 16S rRNA gene sequences, quality-filtered reads were clustered into operational taxonomic units (OTUs) at a 97% similarity threshold using Uparse. Microbial community diversity within samples (alpha diversity) was assessed by calculating indices including Sobs, Chao1, Shannon, ACE, and Simpson based on the rarefied OTU table using the 'vegan' package (v2.6-4) in R [36]. For analyses of vertical variation in community structure and diversity, statistical comparisons were performed only on depth intervals that were consistently sampled across all cored sites. To identify bacterial taxa with significant abundance differences across sediment depths, statistical testing was performed using the Kruskal–Wallis rank-sum test, with post hoc analysis carried out by the Tukey–Kramer method [37].

Relationships between microbial community composition, functional gene abundance, and environmental variables were examined using Spearman correlation analysis. The resulting *p*-values were adjusted for multiple comparisons using the Benjamini–Hochberg false discovery rate (FDR) correction. Correlations with an adjusted p (FDR) < 0.05 were considered statistically significant. Results were visualized as heatmaps. Network analysis was employed to explore co-occurrence patterns among dominant functional categories, and the Random Forest algorithm was used to identify key predictive functions associated with environmental gradients. All statistical analyses and visualizations were performed using SPSS (v27.0), OriginPro (v2022b), and R (v4.2.1). In R, specific analyses and visualizations were conducted using the following packages: 'vegan' (v2.6-4) for community ecology analyses, 'ggplot2' (v3.4.0) and 'pheatmap' (v1.0.12) for generating figures, 'igraph' (v1.4.0) for network analysis, and 'randomForest' (v4.7-1.1) for the Random Forest algorithm.

3. Results and Discussion

3.1. Bacterial Diversity Declines with Sediment Depth Profile

Bacterial species richness showed a clear decline with increasing sediment depth. Surface layers (0–25 cm) sustained the highest diversity (Sobs = 3455 species), which was 1.2 to 1.9 times greater than deeper strata (Table 1). This vertical attenuation (i.e., the decline in diversity with depth) was more pronounced than typically reported in urban sediment systems (where declines are often <1.5-fold) and is mechanistically driven by labile pollutant enrichment (e.g., COD, NH_4^+-N) fueling surface microbial activity, while the strong enrichment of obligate and facultative anaerobic taxa in layers below 50 cm indicates the establishment of predominantly anaerobic conditions, consistent with the typical depletion of oxygen in deeper sediments [10,13,38]. Crucially, such clear stratification contrasts with historically reported minimal depth-related variation in eutrophic riverine overlying water,

highlighting previously overlooked sediment microbial zonation in rural systems [39]. Our data provide strong evidence for deterministic vertical partitioning (i.e., community assembly driven consistently by environmental filtering) in RBOWBs: richness indices (ACE = 4354; Chao1 = 4027) decreased notably with depth (Table 1). The Venn diagram (Figure 1) further illustrates this pattern, showing that only 1310 OTUs were shared across all five depth layers. This small common core, contrasted with the large number of OTUs unique to specific layers (particularly the surface), underscores a high degree of community turnover and strong depth-specific selection of bacterial taxa [40]. Functionally, this stratification reflects a shift from taxa driving carbon hydrolysis and desulfurization in surface layers to anaerobic groups mediating denitrification in deeper anoxic zones [41]. This pattern aligns with the gradients of labile pollutants and oxygen availability. The pronounced vertical partitioning underscores the ecological necessity for depth-resolved remediation strategies in heavily polluted rural aquatic systems [38,39].

Table 1. Vertical gradient of α diversity indices of bacterial community in RBOWBs.

Vertical Gradient	Sobs Index	ACE Index	Chao1 Index	Shannon Index	Simpson Index
A (0~25 cm)	3455	4354	4027	5.96	0.04
B (25~50 cm)	2393	3248	3101	5.12	0.06
C (50~75 cm)	1788	2387	2294	5.07	0.03
D (75~100 cm)	2074	2946	2856	5.16	0.03
E (100~125 cm)	2582	3476	3283	5.77	0.01

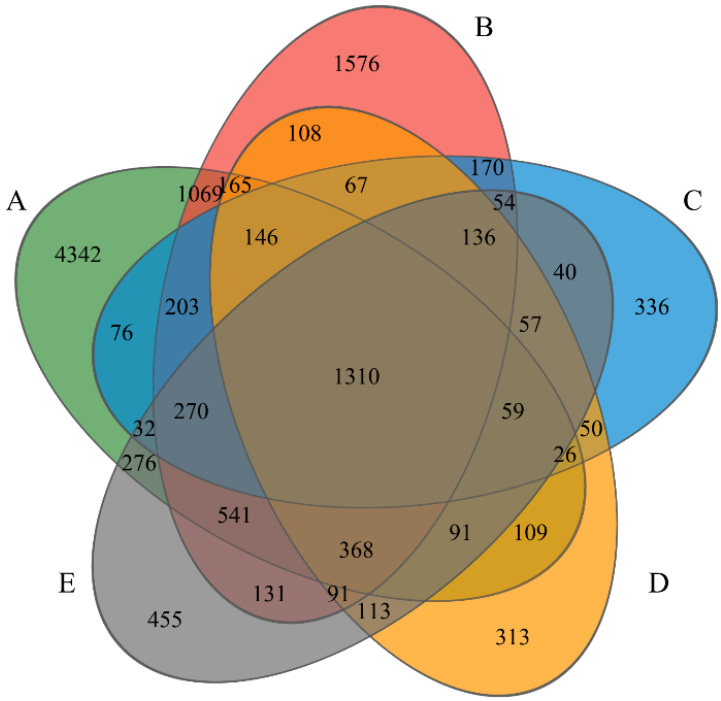


Figure 1. Venn diagram illustrating the shared and unique bacterial OTUs (97% similarity) across five sediment depth layers: A (0–25 cm), B (25–50 cm), C (50–75 cm), D (75–100 cm), and E (100–125 cm).

3.2. Vertical Stratification of Bacterial Community Composition

3.2.1. Phylum-Level Composition Reveals Surface Enrichment of Chloroflexi Linked to Carbon Hydrolysis

Nine bacterial phyla with an average relative abundance exceeding 3% were identified across sediment depths. These dominant phyla were Proteobacteria (20.7–60.4%), Firmicutes (1.7–50.8%), Actinobacteria (4.4–26.1%), Chloroflexi (3.77–14.22%), Acidobacteria (1.43–8.42%), Bacteroidota (0.30–11.70%), Myxococcota (0.51–3.81%), Desulfobacterota

(0.31–3.50%), and Gemmatimonadota (0.13–3.10%) (Figure 2a). Collectively, these nine dominant phyla accounted for 86.12% to 96.00% of all sequences.

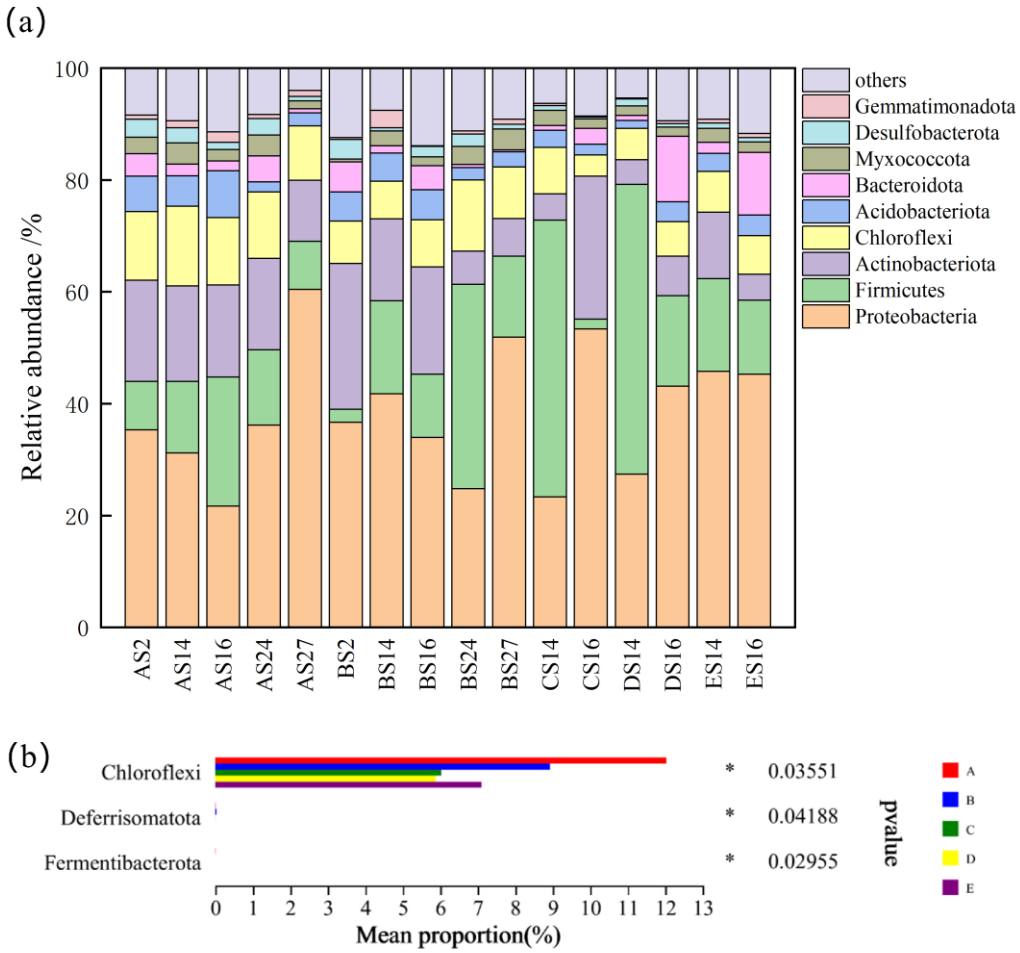


Figure 2. Vertical stratification and differential abundance of sediment bacterial communities at the phylum level. (**a**) Relative abundance of major bacterial phyla across sediment depths. (**b**) Significantly differentially abundant phyla among sediment layers (Kruskal–Wallis test, asterisk (*) indicates significant differences at $p < 0.05$). Sample labels combine the site identifier (e.g., S2) and the corresponding depth interval (e.g., 0–25 cm). AS2, AS14, AS16, AS24, AS27 represent sediment samples from layer A of S2, S14, S16, S24, and S27 in waterbodies, while other indicators indicate similar results.

Significant vertical differentiation in their distribution was observed within the sediment profile. Proteobacteria and Firmicutes were widely distributed across all depths. In contrast, Chloroflexi exhibited significantly higher relative abundance in the surface layer (0–25 cm), averaging 12.0%, which was 2.0 times greater than in deeper layers ($p < 0.05$). This pronounced surface enrichment of Chloroflexi, exceeding typical levels reported in urban sediments (<8%), highlights a distinctive feature of RBOWBs [10,13]. Ecologically, this pattern suggests strong selection for the metabolic traits of Chloroflexi in surface sediments. Members of this phylum are known for their versatility in carbon processing, including the fermentation of sugars and the hydrolysis of complex polysaccharides, which align with the high load of labile and plant-derived organic matter characteristic of rural runoff [42,43]. Their enrichment likely represents a direct microbial response to the surplus of organic carbon in surface sediments, positioning them as key initial processors in the sediment carbon cascade [10]. Actinobacteria abundance was significantly higher in the 0–75 cm depth (mean 15.2%) compared to the bottom layer (5.7%). Acidobacteria showed

an average relative abundance in the surface layer (4.9%) twice that of the bottom layer. Kruskal–Wallis tests revealed extremely significant differences among layers for Chloroflexi, Deferrisomatota, and Fermentibacteria ($p < 0.001$) (Figure 2b).

Consequently, Chloroflexi exhibited the most marked depth-stratified pattern at the phylum level (Kruskal–Wallis, $p < 0.001$; Figures 2b and S1), underscoring its role as a strong bioindicator of the surface sediment environment. This strong differentiation reflects the selective pressure of the surface eutrophic environment (characterized by high COD/NH_4^+-N) favoring heterotrophic and potentially phototrophic members of Chloroflexi [8]. The decline in its abundance with depth likely marks the transition from a carbon- and light-driven (in shallow, turbid water) ecological niche to one dominated by anaerobic respirers and fermenters, illustrating a fundamental shift in energy acquisition strategies along the vertical redox gradient [17]. This highlights the dual regulatory mechanisms of surface nutrient availability versus deep-layer anaerobic constraints. Studies indicate that Chloroflexi can effectively utilize sediment TP_2 and other nutrients, with higher relative abundances correlating with areas richer in pollutants within sediments [24]. Therefore, the vertical zonation of Chloroflexi not only maps the gradient of labile carbon but also may reflect the bioavailability of phosphorus, directly linking its distribution to the primary environmental drivers identified later in our study.

3.2.2. Class-Level Shifts Highlight the Transition from Aerobic Surface Taxa to Anaerobic Denitrifiers with Depth

The relative abundance of bacterial communities at the class level across sediment depths in rural black-odorous waterbodies is presented in Figure 3. The dominant classes were γ-Proteobacteria (12.97–57.54%), Bacilli (0.79–42.08%), Actinobacteria (2.40–19.50%), α-Proteobacteria (1.89–12.31%), and Anaerolineae (1.50–10.48%) (Figure 3).

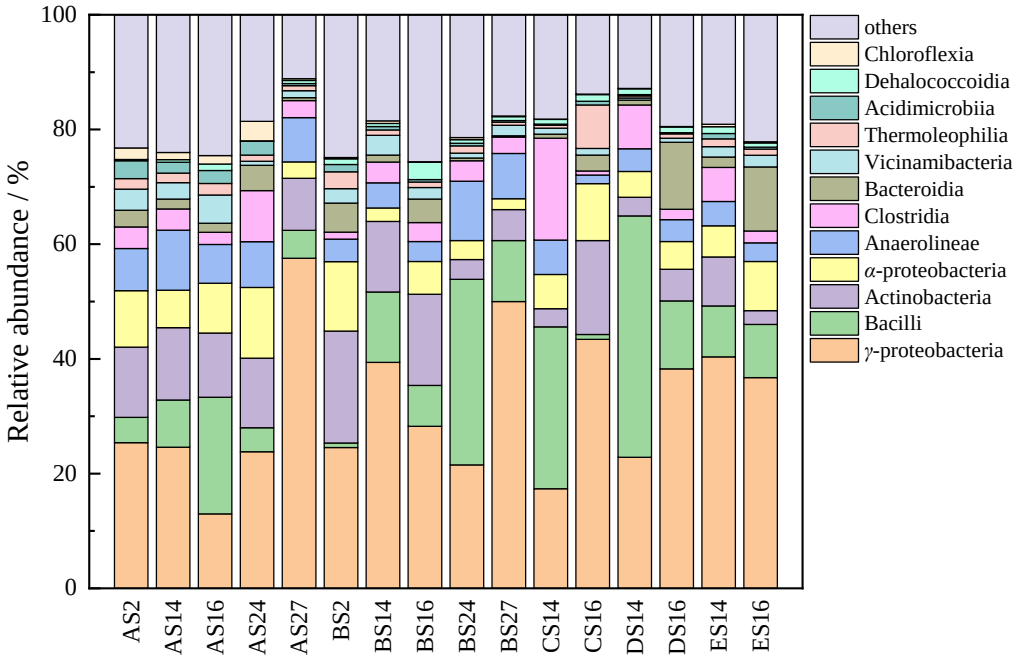


Figure 3. Relative abundance of bacterial community in the sediments at different depths of rural black and odorous waterbodies at class level. Sample labels combine the site identifier (e.g., S2) and the corresponding depth interval (e.g., 0–25 cm). AS2, AS14, AS16, AS24, AS27 represent sediment samples from layer A of S2, S14, S16, S24, and S27 in waterbodies, while other indicators indicate similar results.

The relative abundance of these dominant bacterial classes exhibited distinct vertical trends. γ-Proteobacteria and Bacilli were predominantly accumulated in non-surface sediment layers. This distribution is ecologically coherent with the establishment of anoxic conditions at depth. γ-Proteobacteria encompasses a vast array of facultative and obligate anaerobes capable of diverse respiratory strategies, including denitrification, sulfate reduction, and metal reduction, which become energetically favorable in the absence of oxygen [15,20]. Similarly, the prominence of Bacilli, many of which are fermentative and capable of forming stress-resistant endospores, reflects an adaptive strategy to the harsh, fluctuating, and often toxic (e.g., from sulfide or metals) conditions prevalent in deeper, organic-rich sediments [16,44]. In contrast, Actinobacteria and Anaerolineae were mainly present in the surface and subsurface sediment layers. Actinobacteria are renowned for their capacity to degrade complex organic polymers (e.g., cellulose, chitin), making them key players in the initial breakdown of particulate organic matter entering the sediment [14]. Anaerolineae, a class within the Chloroflexi phylum, are often associated with anaerobic fermentation of carbohydrates, suggesting their role in processing organic carbon in the suboxic transition zone just below the actively reworking surface layer [10].

Significant differences ($p < 0.05$) in the mean relative abundance of bacterial classes were observed across sediment depths. As shown in Figure S2, the mean relative abundance of Chloroflexia, Symbiobacteriia, Blastocatellia, Nitrospiria, and Planctomycetes differed significantly ($p < 0.05$) among depths. This statistical validation reinforces that class-level composition is non-randomly structured by depth. Among these, Chloroflexia, Blastocatellia, Nitrospiria, and Planctomycetes exhibited clear dominance in the A-layer sediment. Chloroflexia and Blastocatellia are implicated in the degradation of recalcitrant organic compounds and atmospheric CO_2 fixation, respectively, highlighting surface-layer processes tied to fresh carbon inputs and potential autotrophic carbon assimilation [45,46]. Nitrospiria includes nitrite-oxidizing bacteria, indicating active nitrogen cycling even in surface sediments. Furthermore, Symbiobacteriia, which possesses functions for cellulose degradation and nitrogen transformation, showed an increasing trend in mean relative abundance with greater sediment depth. This intriguing pattern may point to a symbiotic or syntrophic role in deeper anaerobic layers, perhaps partnering with methanogens or other fermenters to fully mineralize organic matter under strict anaerobic conditions [25].

This functional stratification—carbon hydrolysis and oxidation predominating in surface layers versus fermentation, anaerobic respiration, and syntrophy in middle and deeper layers—is more pronounced than typically observed in urban waterbodies [13,39]. This enhanced stratification is likely a direct consequence of the greater magnitude and different quality (richer in lignocellulosic plant residues) of organic matter inputs in rural catchments, which impose a stronger vertical gradient of electron donors and acceptors, thereby driving more discrete microbial niche partitioning [43,47].

3.2.3. Genus-Level Analysis Identifies Key Depth-Specific Taxa Driving Sulfur, Carbon, and Nitrogen Cycling

Within the sediment profile, the dominant bacterial genera were *Thiobacillus* (0.56–38.35%), *Bacillus* (0.22–36.99%), and *Sideroxydans* (0.14–12.27%) (Figure 4). The composition of these dominant genera varied across the sediment profile. *Thiobacillus* was predominantly concentrated in the surface sediment layer, playing a crucial role in desulfurization and denitrification; it is frequently reported as a dominant genus in sediments of polluted and black-odorous waters [10,17]. In contrast, *Bacillus* and *Sideroxydans* were mainly found in non-surface sediments. *Bacillus*, known for its stress resistance and often found as a dominant group in organically polluted sediments [18], produces spores that aid in surviving heavy metal stress and harsh environmental conditions [16,44]. *Sideroxydans* is significant in iron cycling processes and has been identified as a key iron-oxidizing genus

in anoxic, metal-rich environments [11,14], while *Pseudarthrobacter* primarily participates in sediment carbon and nitrogen cycling, as well as the metabolism of complex organic compounds and proteins [18,48]. The observed differences in dominant genera composition among various rural black-odorous water sediments are likely closely linked to site-specific pollutant sources, such as agricultural runoff (rich in nitrogen and pesticides), domestic sewage (high in organic matter and ammonia), and livestock farming effluents [18,19].

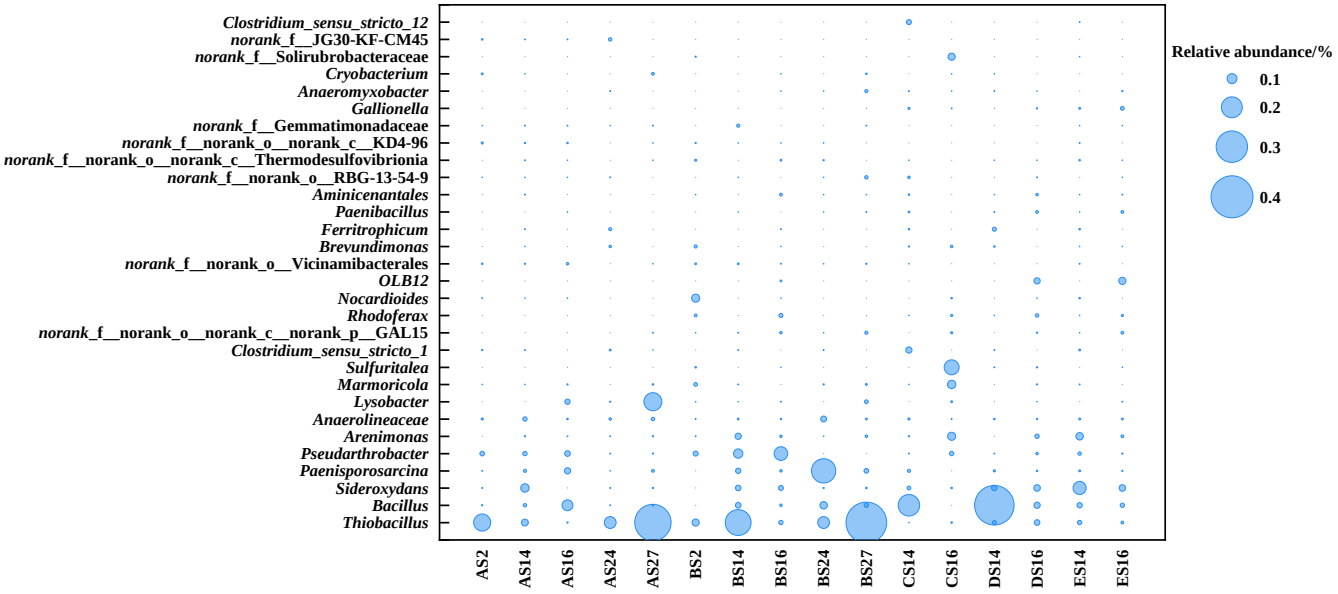


Figure 4. Relative abundance of dominant bacterial genera in the sediments at different depths of rural black and odorous waterbodies. Sample labels combine the site identifier (e.g., S2) and the corresponding depth interval (e.g., 0–25 cm). AS1 represents sediment samples from layer A of sediment in waterbody S1, while other indicators indicate similar results.

Kruskal–Wallis tests indicated significant differences ($p < 0.05$) in the relative abundance of the top 10 differentiating genera across sediment depths (Figure S3). Genera such as *norank_f__JG30-KF-CM45*, *norank_f__Caldilineaceae*, and *Sphingomonas* exhibited their highest mean relative abundances in the surface sediment. *Sphingomonas* is primarily involved in degrading aromatic compounds [49,50]. Conversely, *Gallionella*, *Candidatus Nitrotoga*, *norank_f__Symbiobacteraceae*, and *norank_f__Gallionellaceae* showed higher mean relative abundances in non-surface sediments. *Gallionella* plays an important role in the microbial oxidation of Fe(II) under microaerophilic or anaerobic conditions [17], while *Candidatus Nitrotoga* is mainly involved in nitrogen cycling processes [51]. This stratified cooperative mechanism—characterized by surface desulfurization (*Thiobacillus*), mid-layer carbon fixation (*Pseudarthrobacter*), and deep layer nitrogen fixation (*Candidatus Nitrotoga*)—provides species-specific biomarkers for targeted bioaugmentation.

3.3. Metagenomic Analysis Reveals a Core Functional Repertoire Dominated by Carbohydrate and Amino Acid Metabolism

Each sediment sample subjected to shotgun metagenomic sequencing yielded approximately 15 Gb of high-quality base pairs post-quality control, corresponding to 93.145–113.671 million clean reads (Table S2).

Metagenomic sequencing revealed a core functional repertoire in the sediment bacterial communities dominated by fundamental metabolic processes (Figure 5). The most abundant genes were associated with metabolism (KEGG Level 1), with specific enrichment in Global and Overview Maps, carbohydrate metabolism, and amino acid metabolism (KEGG Level 2) (Figure 5). This pronounced emphasis on core metabolism over specialized

pathways (e.g., xenobiotic degradation) suggests a community primarily geared towards processing abundant, labile organic matter rather than recalcitrant industrial compounds, reflecting the nature of rural pollution sources such as agricultural runoff and domestic sewage [18,19]. At a finer resolution (KEGG Level 3), high abundances of genes involved in metabolic pathways, carbon metabolism, and Biosynthesis of amino acids were detected (Figure 6). This functional profile indicates a microbial community primed for the degradation of complex organic inputs and the synthesis of cellular constituents, a characteristic metabolic strategy in nutrient-rich, heterotrophic ecosystems [50].



Figure 5. Functional profiles of the sediment bacterial communities based on metagenomic analysis (KEGG Level 1 and Level 2). The analysis is based on surface sediment samples.

The analysis of carbohydrate-active enzymes (CAZys) further detailed the community's capacity for polysaccharide metabolism (Figure 7). The parallel prominence of glycosyl transferases (GTs) and glycoside hydrolases (GHs) underscores a high intrinsic potential for the breakdown and transformation of complex carbohydrates. This GT/GH-dominated profile is ecologically coherent with the substantial input of plant-derived polymeric carbon (e.g., cellulose, hemicellulose) from surrounding farmland and vege-

tation into rural waterbodies [43]. Notable abundances of Carbohydrate Esterases (CEs) and Polysaccharide Lyases (PLs) suggest complementary capabilities for degrading pectin (common in plant tissues) and alginate (from algal biomass), respectively. Thus, the CAZy landscape provides a direct functional link between the documented taxonomic shifts (e.g., surface Chloroflexi known for complex carbohydrate degradation) and the predicted carbon flow in these ecosystems.

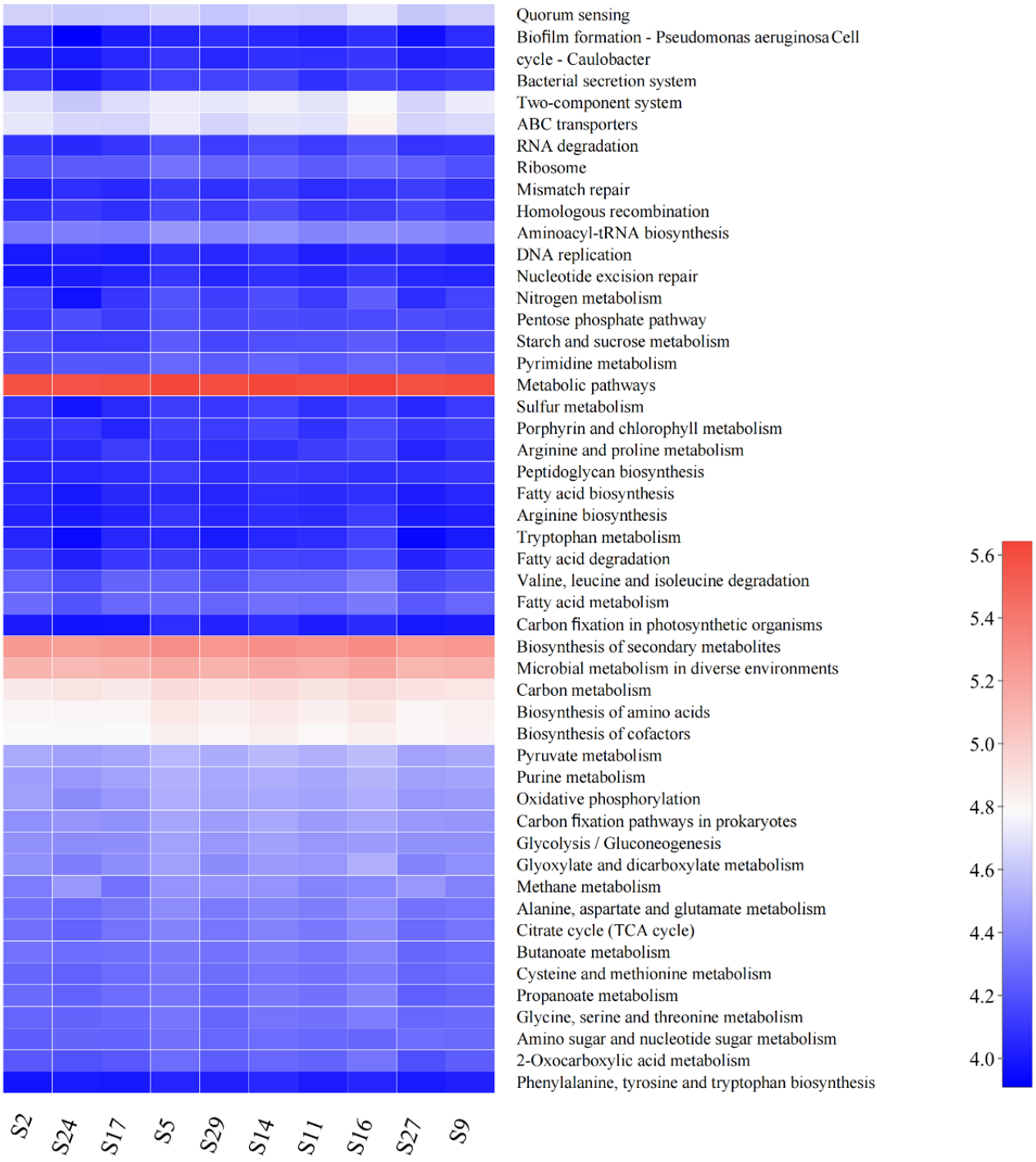


Figure 6. Heatmap of the relative abundance of dominant KEGG pathways at Level 3. The analysis is based on surface sediment samples.

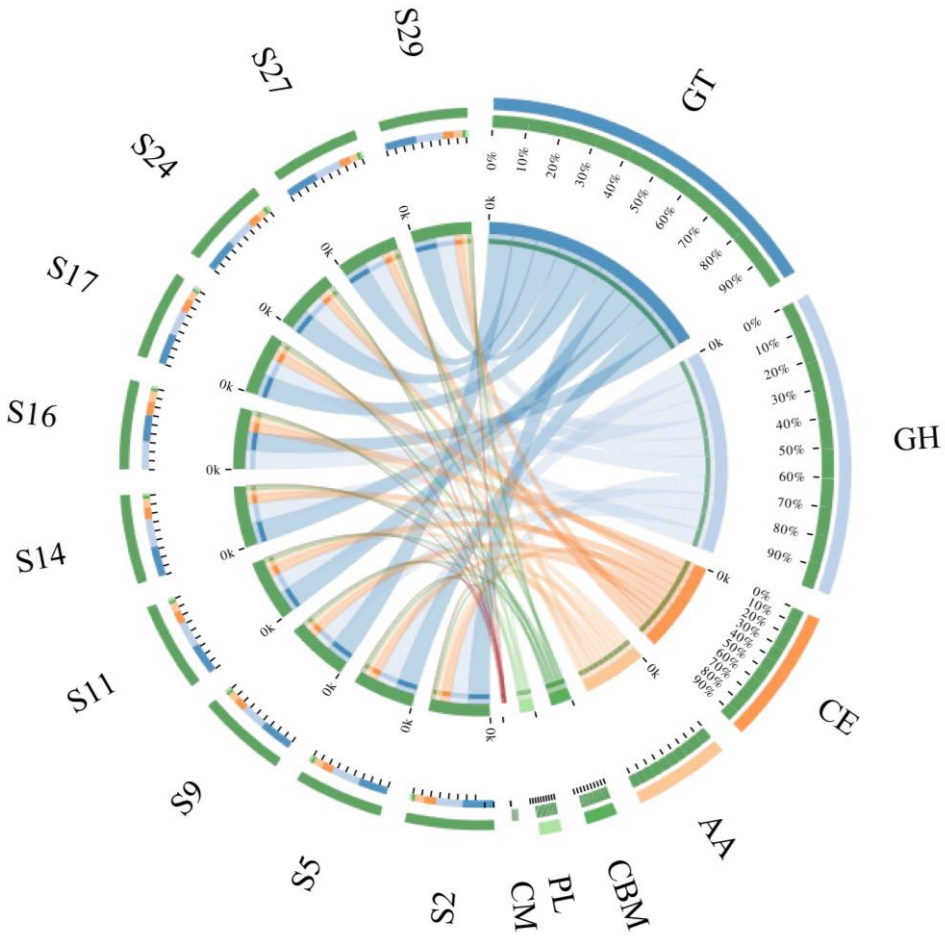


Figure 7. Active enzyme function analysis of CAZy carbohydrate in the sediments of rural black and odorous waterbodies (RPKM). GT: glycosyl transferase, GH: glycoside hydrolase, CE: Carbohydrate Esterase, AAs: Auxiliary Activities, CBMs: Carbohydrate-Binding Modules, PL: Polysaccharide Lyase, CMs: Cellulosome Modules. The analysis is based on surface sediment samples.

The convergence of these core metabolic capabilities—energy generation, nutrient assimilation, and polymer degradation—points to a community optimized for rapid turnover of allochthonous organic matter. This functional configuration supports the 'priming effect' hypothesis, where the influx of labile carbon and nutrients fuels microbial activity that subsequently enhances the processing of more complex native organic matter, potentially accelerating sediment oxygen demand and contributing to the hypoxic/anoxic conditions that underlie black-odor phenomena [20]. Importantly, while this functional potential is high, its expression is likely modulated by the vertical redox gradient, as suggested by the strong correlations between key metabolic pathways and overlying water chemistry (Section 3.4). This functional redundancy and metabolic breadth may confer resilience, allowing the community to maintain core ecosystem processes despite fluctuations in organic input or oxygen levels typical of RBOWBs.

3.4. Overlying Water Chemistry Is Linked to Microbial Functional Potential and Suggests Key Ecological Mechanisms

Correlation analysis (Spearman, with FDR adjustment for multiple comparisons) between CAZy profiles and environmental factors revealed distinct regulatory links (Figure 8). Elevated TP_1 in the overlying water exhibited a significant negative correlation ($p < 0.05$) with the functional potential for polysaccharide degradation, specifically impacting Cellulosome Modules (CMs), glycosyl transferases (GTs), and Polysaccharide Lyases (PLs). This

suggests a potential metabolic trade-off or suppression, where high phosphorus loading, often indicative of eutrophication, may shift microbial investment away from the energetically costly breakdown of complex plant-derived polymers towards the utilization of more labile substrates, or may reflect broader community stress under hyper-eutrophic conditions [17]. Conversely, alkaline pH conditions in the waterbody showed a significant positive correlation ($p < 0.05$) with the functional potential of Carbohydrate-Binding Modules (CBMs) and GH. Alkalinity likely enhances the stability and catalytic efficiency of many extracellular hydrolytic enzymes, and may also favor the activity of specific bacterial taxa adept at polysaccharide decomposition under such conditions [14,48]. Crucially, the lack of significant correlation with sediment nutrients underscores that the immediate functional blueprint of the sediment microbiome is more responsive to the dynamic chemical milieu of the overlying water, which acts as a primary vector of pollutants and a mediator of redox conditions at the sediment–water interface. Notably, the negative correlation between arsenic (As) and CM (Figure 8) suggests that As stress may suppress the microbial investment in extracellular degradation of complex carbohydrates, reflecting a potential metabolic trade-off under metal pressure [52].

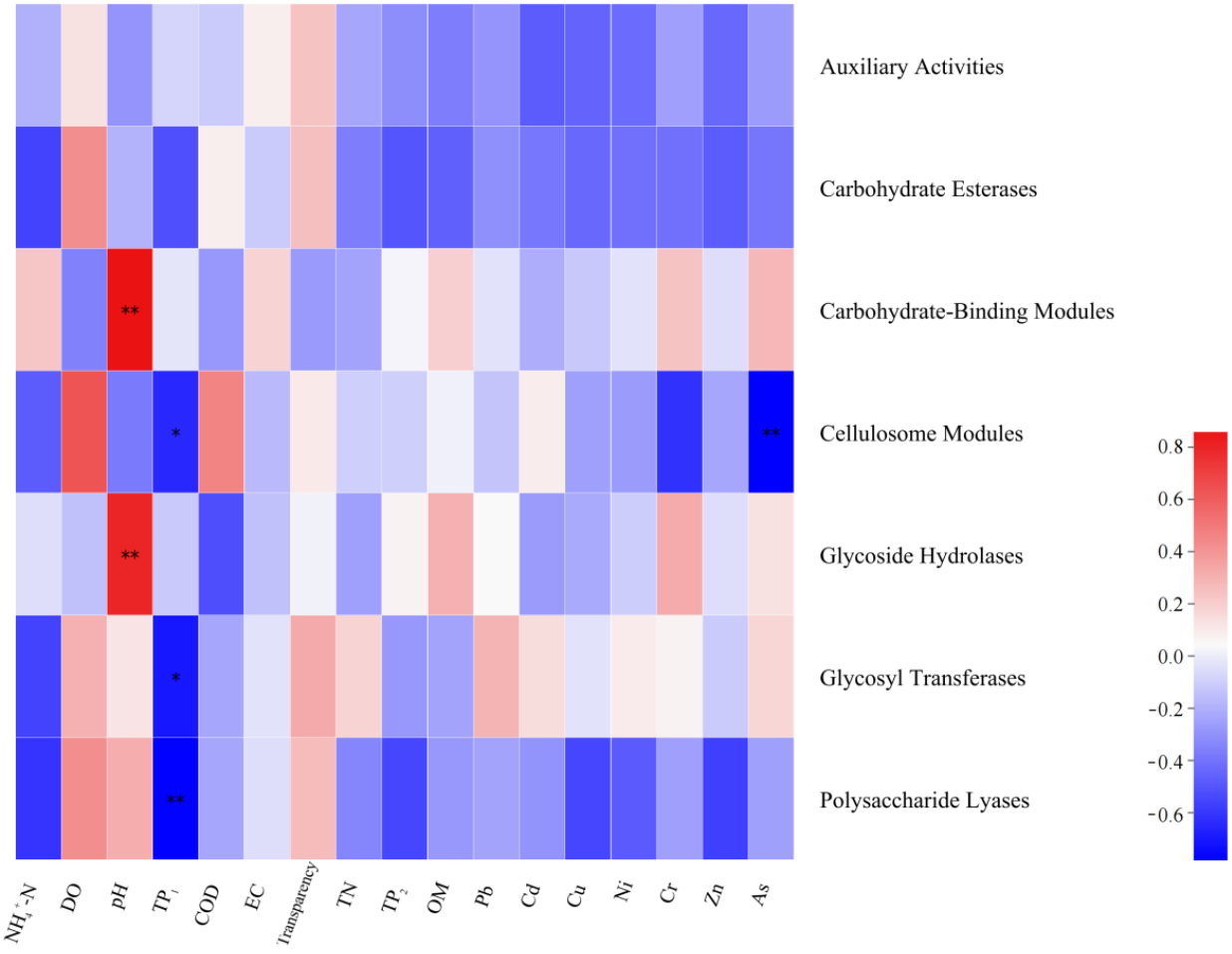


Figure 8. Correlation between active enzymes of CAZy carbohydrate and environmental factors in the sediments of rural black and odorous waterbodies. Spearman correlation analysis was performed, and *p*-values were adjusted for multiple comparisons using the Benjamini–Hochberg false discovery rate (FDR) correction. The color bar represents correlation, red represents positive correlation, and blue represents negative correlation; * indicates FDR-adjusted $p < 0.05$, ** indicates FDR-adjusted $p < 0.01$.

Further analysis of KEGG Level 3 metabolic functions (top 50 based on RPKM) revealed strong regulatory links between overlying water factors and core microbial metabolism (Figure 9). Key pathways, including nitrogen metabolism, sulfur metabolism, carbon metabolism, showed significant positive correlations (FDR-adjusted $p < 0.05$) with overlying water TP_1 and pH. The link with TP_1 may reflect phosphorus serving not only as a nutrient but also as a signal in regulatory networks governing microbial growth and metabolic investment in these nutrient-rich systems [53]. In stark contrast, DO negatively correlated ($p < 0.05$) with carbon fixation and general carbon metabolism. This inverse relationship highlights the community's metabolic shift towards fermentation and anaerobic respiration under low-oxygen conditions, which is a hallmark of black-odorous ecosystems and directly fuels the production of reduced, odorous compounds [54]. Furthermore, the positive correlations of chromium (Cr) and arsenic (As) with the mismatch repair pathway (Figure 9) likely reflect an adaptive genomic response to metal-induced DNA damage, underscoring the selective pressure exerted by these pervasive contaminants.

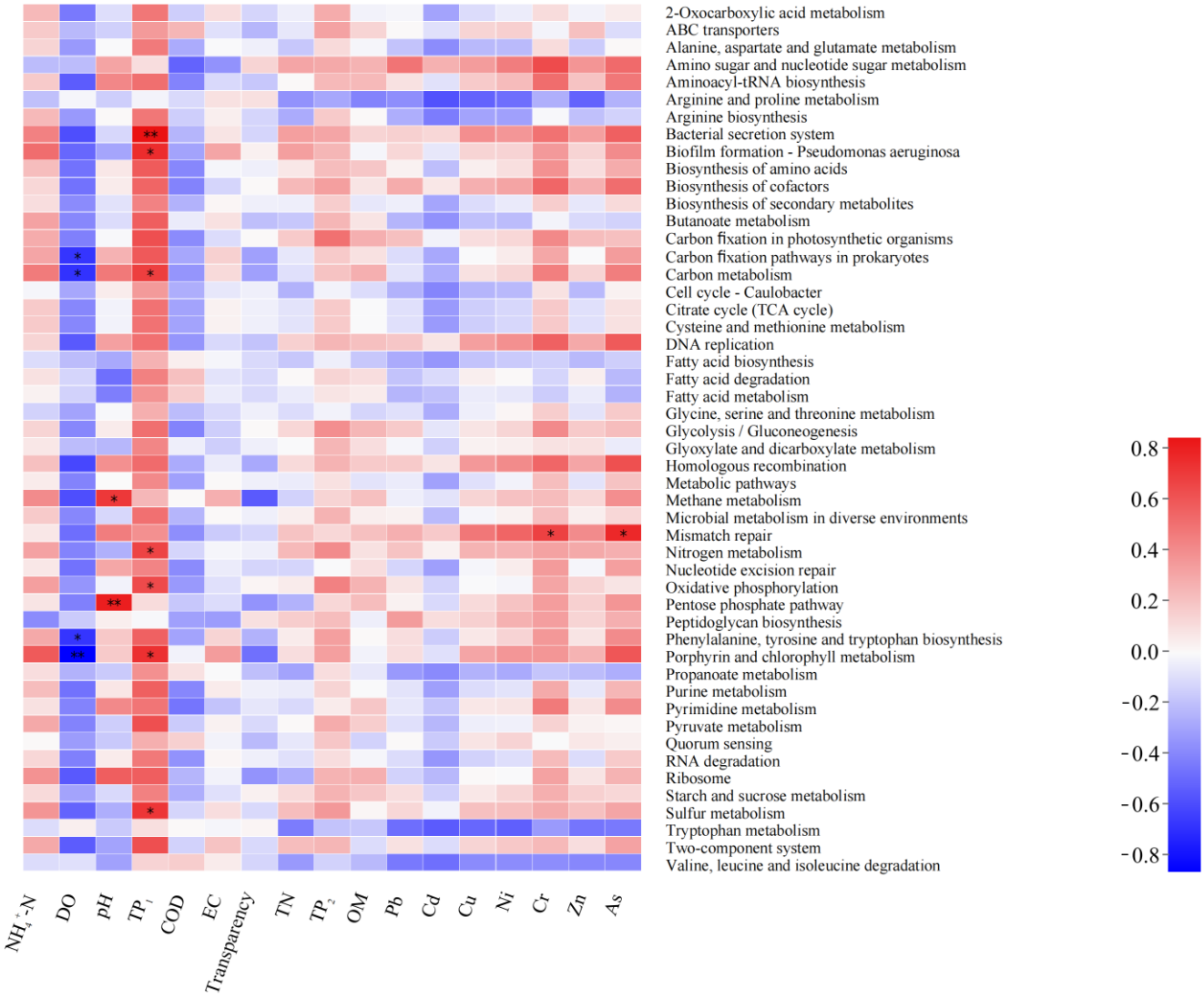


Figure 9. Correlation between the top 50 functional abundance (based on RPKM) and environmental factors based on KEGG Level 3 in the sediments of rural black and odorous waterbodies. Spearman correlation analysis was performed, and *p*-values were adjusted for multiple comparisons using the Benjamini–Hochberg false discovery rate (FDR) correction. The color bar represents correlation, red represents positive correlation, and blue represents negative correlation; * indicates FDR-adjusted $p < 0.05$, ** indicates FDR-adjusted $p < 0.01$.

Synthesizing these correlations with our taxonomic and genetic data, we propose a refined mechanistic model for black-odor generation centered on a vertically stratified sulfur–iron coupling cycle, driven by overlying water chemistry. The surface enrichment of *Thiobacillus* (equipped with sulfur-oxidation genes like *soxB*) and the positive correlation of sulfur metabolism with pH/TP_1 suggest active oxidative zones at the sediment surface, fueled by overlying water inputs. In contrast, the deeper layer abundance of Desulfobacterota (carrying *dsrB* genes) and iron-cycling genera like *Sideroxydans* and *Gallionella*, coupled with the anaerobic conditions indicated by low DO correlation, establishes a reductive engine [20]. We hypothesize that this spatial decoupling creates a diffusion-driven biogeochemical reactor [55]: Sulfate and iron oxides are reduced in the anaerobic depths, producing soluble Fe^{2+} and S^{2-}. These reduced species diffuse upwards, where at the oxic–anoxic interface (influenced by overlying water DO and pH), they react abiotically and through microbial oxidation to form black FeS precipitates and release gaseous H_2S. Thus, the overlying water parameters (TP_1, DO, pH) do not merely correlate with static functional potential; they dynamically regulate the rates and spatial positioning of these coupled redox transformations, thereby controlling the flux of black-odor precursors [56].

This interpretation, while supported by strong correlative patterns and consistent with established biogeochemical principles, highlights the need for future research employing controlled manipulations (e.g., mesocosm experiments with adjusted TP_1/DO) and direct activity measurements (e.g., radiolabeled sulfate reduction rates) to move beyond correlation and definitively establish causality within this proposed mechanistic framework.

4. Conclusions

This study systematically reveals significant depth-dependent differentiation of bacterial communities in the sediments of RBOWBs. The key findings are as follows: (1) Bacterial species richness showed a marked decline with depth, with surface layers (0–25 cm) exhibiting 1.2–1.9 times greater richness than deeper strata. (2) Community composition displayed clear vertical stratification: surface sediments were enriched with taxa like Chloroflexi and *Thiobacillus* linked to carbon hydrolysis and desulfurization, whereas middle and deeper layers were dominated by anaerobic genera such as *Bacillus* and *Candidatus Nitrotoga* involved in denitrification and nitrogen cycling. (3) Metagenomic analysis revealed a core functional potential dominated by carbohydrate and amino acid metabolism. (4) Correlation analysis identified TP_1, DO, and pH of the overlying water—rather than intrinsic sediment nutrients—as the primary environmental factors associated with this vertical microbial zonation and functional potential. These findings demonstrate that neglecting the vertical heterogeneity of sediment microbiota leads to an incomplete understanding of black-odor formation mechanisms. The vertical functional zonation, particularly the suggested sulfur–iron coupling cycle mediated by stratified microbial taxa, provides a mechanistic rationale for future research into the ecological processes underlying pollutant transformation and symptom persistence in these systems.

Building on these insights, future work should focus on the interaction mechanisms among key microbial taxa across different depths, particularly their functional linkages within sulfur–iron–nitrogen coupling cycles. Integrating meta-transcriptomic and metabolomic techniques is necessary to move beyond genetic potential and quantify in situ microbial activities along the depth gradient. Furthermore, the results provide a theoretical foundation for developing targeted microbial remediation strategies. Future research should explore the feasibility of stratified approaches—for instance, by investigating the synergy between surface and deep-layer interventions—while explicitly addressing practical challenges related to inoculant survival, delivery methods, and long-term efficacy

at field scale. Ultimately, by clarifying the ecological functions of microbial vertical zonation and its environmental drivers, this work furnishes targeted scientific support for the long-term management and ecological restoration of RBOWBs.

While this study provides clear evidence of vertical zonation in sediment bacterial communities, several limitations should be considered. First, the findings are based on samples from a specific region (Dongming County, Shandong) during a single season (August). The microbial communities and their drivers might exhibit temporal dynamics (e.g., seasonal variations) and spatial heterogeneity across different geographic regions with distinct pollution sources. Second, our functional analysis relied on metagenomic predictions (potential), which may not fully reflect in situ microbial activity. Integrating meta-transcriptomic or enzymatic activity measurements in future work would strengthen the functional insights. Thirdly, the inability to retrieve full sediment cores at all sites may constrain the resolution of vertical comparisons in some locations. Finally, the study identifies statistical correlations between environmental factors and microbial communities; controlled mechanistic experiments are needed to definitively establish causality in these complex interactions.

Supplementary Materials: The following supporting information can be downloaded at https://www.mdpi.com/article/10.3390/su18031588/s1.

Author Contributions: Conceptualization, Y.T. and X.L.; methodology, Y.T., H.R., and S.L.; software, J.L.; validation, Y.T. and J.W.; formal analysis, Y.T.; investigation, H.R. and J.L.; resources, J.L. and X.L.; data curation, Y.T. and H.R.; writing—original draft preparation, Y.T., H.R., and S.L.; writing—review and editing, Y.T. and S.L.; visualization, H.R.; supervision, X.L.; project administration, X.L.; funding acquisition, X.L., Y.T., and S.L. contributed equally to this work. All authors have read and agreed to the published version of the manuscript.

Funding: This research was funded by the Beijing Municipal Natural Science Foundation, grant No. 8182058).

Institutional Review Board Statement: Not applicable.

Informed Consent Statement: Not applicable.

Data Availability Statement: The raw sequencing data are not currently available for public deposition due to being part of an ongoing project under national patent review (Beijing Municipal Natural Science Foundation, Grant No. 8182058). However, all processed data necessary to reproduce the analyses, figures, and tables presented in this study are included as Supplementary Materials. The full datasets are available from the corresponding author upon reasonable request, subject to a data use agreement, for academic purposes.

Conflicts of Interest: The authors declare no conflicts of interest.

References

1. Peng, K.; Dong, C.; Mi, J. Dynamic Research on the Collaborative Governance in Urban. *Systems* **2024**, *12*, 307. [CrossRef]
2. Shao, Y.; He, Q.; Fu, Y.; Liu, Y. Construction of the Comprehensive Evaluation System of Waterbody Pollution Degree and the Response of Sedimentary Microbial Community. *Environ. Pollu* **2023**, *317*, 120837. [CrossRef]
3. Liang, Z.; Abdillah, A.; Fang, W.; Qiu, R.; Mai, B.; He, Z.; Juneau, P.; Gomes, M.P.; Priadi, C.R.; Wang, S. Unique Microbiome in Organic Matter–Polluted Urban Rivers. *Glob. Change Biol.* **2023**, *29*, 391–403. [CrossRef]
4. Zhang, W.; Zhou, H.; Sheng, R.; Qin, H.; Hou, H.; Liu, Y.; Chen, A.; Chen, C.; Wei, W. Differences in the Nitrous Oxide Emission and the Nitrifier and Denitrifier Communities among Varying Aggregate Sizes of an Arable Soil in China. *Geoderma* **2021**, *389*, 114970. [CrossRef]
5. Liu, Q.; Wu, H.; Huang, C.; Lin, H.; Li, W.; Zhao, X.; Li, Z.; Lv, S. Microbial Compositions, Ecological Networks, and Metabolomics in Sediments of Black-Odour Water in Dongguan, China. *Environ. Res.* **2022**, *210*, 112918. [CrossRef]

6. Pascazio, S.; Crecchio, C.; Scagliola, M.; Mininni, A.N.; Dichio, B.; Xiloyannis, C.; Sofo, A. Microbial-Based Soil Quality Indicators in Irrigated and Rainfed Soil Portions of Mediterranean Olive and Peach Orchards under Sustainable Management. *Agric. Water Manag.* **2018**, *195*, 172–179. [CrossRef]
7. Zhang, W.; Li, Y.; Wang, C.; Wang, P.; Hou, J.; Yu, Z.; Niu, L.; Wang, L.; Wang, J. Modeling the Biodegradation of Bacterial Community Assembly-Linked Antibiotics in River Sediment Using a Deterministic-Stochastic Combined Model. *Environ. Sci. Technol.* **2016**, *50*, 8788–8798. [CrossRef] [PubMed]
8. Huang, H.; Liu, J.; Zhang, F.; Zhu, K.; Yang, C.; Xiang, Q.; Lei, B. Characteristics of Planktonic and Sediment Bacterial Communities in a Heavily Polluted Urban River. *PeerJ* **2021**, *9*, e10866. [CrossRef]
9. Wanek, A.S.; Hargiss, C.L.M.; Norland, J. Assessment of Water Quality in Ponds across the Rural, Peri-Urban, and Urban Gradient. *Environ. Monit. Assess.* **2021**, *193*, 694. [CrossRef] [PubMed]
10. Zhang, D.; Yang, H.; Lan, S.; Wang, C.; Li, X.; Xing, Y.; Yue, H.; Li, Q.; Wang, L.; Xie, Y. Evolution of Urban Black and Odorous Water: The Characteristics of Microbial Community and Driving-Factors. *J. Environ. Sci.* **2022**, *112*, 94–105. [CrossRef] [PubMed]
11. Zhu, J.; Zhang, J.; Li, Q.; Han, T.; Xie, J.; Hu, Y.; Chai, L. Phylogenetic Analysis of Bacterial Community Composition in Sediment Contaminated with Multiple Heavy Metals from the Xiangjiang River in China. *Mar. Pollut. Bull.* **2013**, *70*, 134–139. [CrossRef]
12. Liu, C.; Yang, Y.; Zhou, J.; Chen, Y.; Zhou, J.; Wang, Y.; Fu, D. Migration and Transformation of Nitrogen in Sediment–Water System within Storm Sewers. *J. Environ. Manag.* **2021**, *287*, 112355. [CrossRef]
13. Zhang, H.; Yin, A.; Yang, X.; Wu, P.; Fan, M.; Wu, J.; Zhang, M.; Gao, C. Changes in Surface Soil Organic/Inorganic Carbon Concentrations and Their Driving Forces in Reclaimed Coastal Tidal Flats. *Geoderma* **2019**, *352*, 150–159. [CrossRef]
14. Yao, Y.; Zhao, J.; Miao, L.; Hou, J. Effects of Sediment Physicochemical Factors and Heavy Metals on the Diversity, Structure, and Functions of Bacterial and Fungal Communities from a Eutrophic River. *Environ. Pollut.* **2022**, *303*, 119129. [CrossRef]
15. Zhong, J.; Chen, C.; Yu, J.; Shen, Q.; Liu, C.; Fan, C. Effect of Dredging and Capping with Clean Soil on the Mitigation of Algae-Induced Black Blooms in Lake Taihu, China: A Simulation Study. *J. Environ. Manag.* **2022**, *302*, 114106. [CrossRef] [PubMed]
16. Qian, Y.; Xu, M.; Deng, T.; Hu, W.; He, Z.; Yang, X. Synergistic Interactions of Desulfovibrio and Petrimonas for Sulfate-Reduction Coupling Polycyclic Aromatic Hydrocarbon Degradation. *J. Hazard. Mater.* **2021**, *407*, 124385. [CrossRef]
17. Jing, Z.; Ye, F.; Liu, X.; Gao, H. Review Article A Critical Review of Microbial Profiles in Black and Odorous Waters. *Environ. Res.* **2025**, *270*, 120972. [CrossRef] [PubMed]
18. Cao, J.; Sun, Q.; Zhao, D.; Xu, M.; Shen, Q.; Wang, D.; Wang, Y.; Ding, S. A Critical Review of the Appearance of Black-Odorous Waterbodies in China and Treatment Methods. *J. Hazard. Mater.* **2020**, *385*, 121511. [CrossRef]
19. Ma, J.; Wang, H.; Feng, H.; Li, A.; Guo, X.; Bai, Y. Study on Microbial Community Structure and Functional Characteristics of Typical Rural Black and Odorous Water Bodies in Qingdao. *J. Environ. Eng. Technol.* **2024**, *14*, 464–473.
20. Liang, Z.; Fang, W.; Luo, Y.; Lu, Q.; Juneau, P.; He, Z.; Wang, S. Mechanistic Insights into Organic Carbon-Driven Water Blackening and Odorization of Urban Rivers. *J. Hazard. Mater.* **2021**, *405*, 124663. [CrossRef]
21. Ren, H.; Tian, Y.; Lu, J.; Shi, Y.; Wang, J.; Yue, Z.; Liu, X. Characteristics of Bacterial Community Structure in the Sediment of Rural Black and Odorous Water Bodies. *Environ. Sci.* **2023**, *44*, 6205–6214. [CrossRef]
22. Tian, W.; Zhang, X.; Xu, W.; Wu, L.; Huang, Z.; Cai, Y. Application of Solid-Waste Derived Biochar from Penaeus Vannamei Mariculture for Black-Odorous Water Remediation. *J. Water Process Eng.* **2025**, *75*, 107878. [CrossRef]
23. Rho, T.; Choi, S.; Kim, E.S.; Kang, N.Y.; Cho, S.R.; Khang, S.H. Optimization of Chemical Oxygen Demand Determination in Seawater Samples Using the Alkaline Potassium Permanganate Method. *Ocean Sci. J.* **2018**, *53*, 611–619. [CrossRef]
24. Zhao, X.; Zhao, C.; Stahr, K.; Kuzyakov, Y.; Wei, X. The Effect of Microorganisms on Soil Carbonate Recrystallization and Abiotic CO2 Uptake of Soil. *Catena* **2020**, *192*, 104592. [CrossRef]
25. Yang, C.; Liu, C.; Yan, Y.; Lu, L.; Ma, R.; Xiao, X.; Yu, Y.; Zhao, Y.; Yu, Y.; Li, L. Ecotoxicology and Environmental Safety Efficient Removal of Tris (2-Chloroethyl) Phosphate by Biochar Derived from Shrimp Shell: Adsorption Performance and Mechanism Study. *Ecotoxicol. Environ. Saf.* **2023**, *254*, 114728. [CrossRef]
26. Wen, Y.; Zhang, W.; Shan, B. Amino Acids as Indicators of Seasonal Variations in Organic Matter Degradation in Surface Sediments from a Shallow Lake. *J. Environ. Sci.* **2023**, *131*, 1–10. [CrossRef]
27. Ji, P.; Chen, J.; Chen, F. Nitrogen and Phosphorus Trends in Lake Sediments of China May Diverge. *Nat. Commun.* **2024**, *15*, 2644. [CrossRef] [PubMed]
28. Li, Y.; Zhu, Y.; Chen, Y.; Wang, C.; Zhao, G.; Pan, H.; Wang, C.; Bao, H.; Ibrahim, M.; Norgbey, E. Heavy Metals Contamination in Water-Sediment Systems of a Large Drinking Water Reservoir in Southern China: Large-Scale Assessment and Risk-Based Management. *J. Clean. Prod.* **2025**, *525*, 146557. [CrossRef]
29. Wang, S.; Li, X.; Jiang, X.; Zhang, Y.; Zhang, J.; Liu, Y.; Guo, H.; Li, Z.; Fu, Z. The Interaction between Nutrients and Heavy Metals in Lakes and Rivers Entering Lakes. *Ecol. Indic.* **2024**, *161*, 111963. [CrossRef]

30. Zhang, M.; Hu, Y.; Ma, Y.; Hou, T.; Wang, J.; Che, Q.; Chen, B.; Wang, Q. Soil Bacterial Diversity and Community Structure of Cotton Rhizosphere under Mulched Drip- Irrigation in Arid and Semi-Arid Regions of Northwest China. *Microb. Ecol.* **2025**, *88*, 1–18. [CrossRef] [PubMed]
31. Chen, S.; Zhou, Y.; Chen, Y.; Gu, J. Fastp: An Ultra-Fast All-in-One FASTQ Preprocessor. *Bioinformatics* **2018**, *34*, i884–i890. [CrossRef]
32. Li, D.; Luo, R.; Liu, C.; Leung, C.; Ting, H. MEGAHIT v1.0: A Fast and Scalable Metagenome Assembler Driven by Advanced Methodologies and Community Practices. *Methods* **2023**, *102*, 3–11. [CrossRef]
33. Fu, L.; Niu, B.; Zhu, Z.; Wu, S.; Li, W. BIOINFORMATICS APPLICATIONS NOTE Sequence Analysis CD-HIT: Accelerated for Clustering the next-Generation Sequencing Data. *Bioinformatics* **2012**, *28*, 3150–3152. [CrossRef]
34. Kanehisa, M.; Goto, S. KEGG: Kyoto Encyclopedia of Genes and Genomes. *Nucleic Acids Res.* **2000**, *28*, 27–30. [CrossRef]
35. Lombard, V.; Ramulu, H.G.; Drula, E.; Coutinho, P.M.; Henrissat, B. The Carbohydrate-Active Enzymes Database (CAZy) in 2013. *Nucleic Acids Res.* **2014**, *42*, 490–495. [CrossRef] [PubMed]
36. Sun, H.; Wang, L.; Kumar, A.; Auwal, M.; Van Zwieten, L.; Ge, T.; Fu, Y.; Kuzyakov, Y. Geoderma Nutrient Availability Mediates Organic Carbon Turnover in Paddy Soils through Regulating Microbial Metabolism. *Geoderma* **2025**, *458*, 117313. [CrossRef]
37. Kim, J.H.; Jobbágy, E.G.; Richter, D.D.; Trumbore, S.E.; Jackson, R.B. Agricultural Acceleration of Soil Carbonate Weathering. *Glob. Chang. Biol.* **2020**, *26*, 5988–6002. [CrossRef] [PubMed]
38. Böer, S.I.; Hedtkamp, S.I.C.; Van Beusekom, J.E.E.; Fuhrman, J.A.; Boetius, A.; Ramette, A. Time- and Sediment Depth-Related Variations in Bacterial Diversity and Community Structure in Subtidal Sands. *ISME J.* **2009**, *3*, 780–791. [CrossRef]
39. Gao, Y.; Wang, C.; Zhang, W.; Di, P.; Yi, N.; Chen, C. Vertical and Horizontal Assemblage Patterns of Bacterial Communities in a Eutrophic River Receiving Domestic Wastewater in Southeast China. *Environ. Pollut.* **2017**, *230*, 469–478. [CrossRef]
40. Tai, X.; Li, R.; Zhang, B.; Yu, H.; Kong, X.; Bai, Z.; Deng, Y.; Jia, L. Pollution Gradients Altered the Bacterial Community Composition and Stochastic Process of Rural Polluted Ponds. *Microorganisms* **2020**, *8*, 311. [CrossRef]
41. Tang, X. Vertical Spatial Denitri Fi Cation Performance and Microbial Community Composition in Denitri Fi Cation Bio Fi Lters Coupled with Water. *RSC Adv.* **2024**, *14*, 15431–15440. [CrossRef]
42. Ma, T.; Zhu, S.; Wang, Z.; Chen, D.; Dai, G.; Feng, B.; Su, X.; Hu, H.; Li, K.; Han, W.; et al. Divergent Accumulation of Microbial Necromass and Plant Lignin Components in Grassland Soils. *Nat. Commun.* **2018**, *9*, 3480. [CrossRef] [PubMed]
43. Wang, G.; Li, X.; Fang, Y.; Huang, R. Analysis on the Formation Condition of the Algae-Induced Odorous Black Water Agglomerate. *Saudi J. Biol. Sci.* **2014**, *21*, 597–604. [CrossRef]
44. Hu, A.; Ju, F.; Hou, L.; Li, J.; Yang, X.; Wang, H.; Mulla, S.I.; Sun, Q. Strong Impact of Anthropogenic Contamination on the Co-Occurrence Patterns of a Riverine Microbial Community. *Environ. Microbiol.* **2017**, *19*, 4993–5009. [CrossRef]
45. Fa, K.; Liu, Z.; Zhang, Y.; Qin, S.; Wu, B.; Liu, J. Abiotic Carbonate Dissolution Traps Carbon in a Semiarid Desert. *Sci. Rep.* **2016**, *6*, 23570. [CrossRef] [PubMed]
46. Huber, K.J.; Geppert, A.M.; Groß, U.; Luckner, M.; Wanner, G.; Cooper, P.; Abakah, J.; Janssen, I.; Overmann, J. *Aridibacter Nitratireducens* sp. nov., a Member of the Family *Blastocatellaceae*, Class *Blastocatellia*, Isolated from an African Soil. *Int. J. Syst. Evol. Microbiol.* **2017**, *67*, 4487–4493. [CrossRef] [PubMed]
47. Jing, Z.; Li, Q.; Wei, Y.; Dong, B.; Yuan, P.; Liu, R. Mechanistic Insights into Dissolved Organic Matter-Driven Protistan and Bacterial Community Dynamics Influenced by Vegetation Restoration. *Environ. Res.* **2023**, *227*, 115710. [CrossRef]
48. Zhang, L.; Huang, S.; Peng, X.; Liu, B.; Zhang, X.; Ge, F. Potential Ecological Implication of Cladophora Oligoclora Decomposition: Characteristics of Nutrient Migration, Transformation, and Response of Bacterial Community Structure. *Water Res.* **2021**, *190*, 116741. [CrossRef]
49. Liu, S.; Zhou, A.; Fan, Y.; Duan, Y.; Liu, W.; Yue, X. Science of the Total Environment Using Heat-Activated Persulfate to Accelerate Short-Chain Fatty Acids Production from Waste Activated Sludge Fermentation Triggered by Sulfate-Reducing Microbial Consortium. *Sci. Total Environ.* **2023**, *861*, 160795. [CrossRef]
50. Zhang, H.; Li, S.; Li, M.; Duan, L.; Zhang, H.; Qin, W.; Zhao, L.; Liu, P.; Lü, Y.; Wang, Y. Carbon Emission Analysis of Municipal Wastewater Treatment Plants and Discussion on Synergistic Path of Pollution and Carbon Reduction. *J. Environ. Eng. Technol.* **2023**, *13*, 2053–2062. [CrossRef]
51. Spieck, E.; Wegen, S.; Keuter, S. Relevance of *Candidatus Nitrotoga* for Nitrite Oxidation in Technical Nitrogen Removal Systems. *Appl. Microbiol. Biotechnol.* **2021**, *105*, 7123–7139. [CrossRef] [PubMed]
52. Chou, W.; Chen, H.; Yu, S.; Cheng, L.; Yang, P.; Dang, C.V. Arsenic Suppresses Gene Expression in Promyelocytic Leukemia Cells Partly through Sp1 Oxidation. *Blood* **2005**, *106*, 304–310. [CrossRef]
53. Wu, Y.; Wang, W.; Liu, X.; Sheng, Y. Functional Microorganisms Drive the Formation of Black-Odorous Water. *Microorganisms* **2024**, *12*, 487. [CrossRef]
54. Shi, Y.; Wei, Z.; Xu, Y.; Lu, X.; Ruan, A. Effects of Electrochemical Intervention on the Remediation of Black-Odorous Water: Insights into Microbial Community Dynamics and Functional Shifts in Sediments. *Water Sci. Technol.* **2023**, *87*, 2776–2792. [CrossRef] [PubMed]

55. Ni, R.; Yang, Q.; Wang, B.; Li, G.; Zhao, J.; Zhang, H.; Zhang, X.; Fang, W.; Xu, D.; Gong, H.; et al. Composite Modified Clay Mineral Integrated with Microbial Active Components for Restoration of Black-Odorous Water. *Sustainability* **2026**, *18*, 33. [CrossRef]
56. Li, L.; Zhang, Z.; Shen, Y.; He, B.; Fu, Y.; Kou, S.; Gao, J. Optimized Design of Modular Constructed Wetland for Treating Rural Black—Odorous Water. *Water* **2024**, *16*, 2492. [CrossRef]

Disclaimer/Publisher's Note: The statements, opinions and data contained in all publications are solely those of the individual author(s) and contributor(s) and not of MDPI and/or the editor(s). MDPI and/or the editor(s) disclaim responsibility for any injury to people or property resulting from any ideas, methods, instructions or products referred to in the content.